Impact of large tip clearance ratios on the performance of a centrifugal compressor

M. Diehl - J. Schiffmann

LAMD, EPF Lausanne, Switzerland, markus.diehl@epfl.ch, jurg.schiffmann@epfl.ch

ABSTRACT

Ultra-compact and fast spinning turbomachinery is a key technology to increase performance of domestic heating applications and to address decentralization of power and heat as a consequence of the rise of renewable energy sources. Recently, a heat pump using a reduced-scale centrifugal compressor with an impeller diameter of 20 mm supported on gas bearings was tested successfully and higher system performance compared to commonly used positive displacement compressors was achieved. Nonetheless, due to the small feature size as well as manufacturing tolerances, the performance of such compressor systems is deteriorated compared to large-scale systems. The tip gap necessary to ensure a free spinning of the rotor on gas bearings is relatively large compared to industrial compressors.
Unfortunately, limited experience about centrifugal compressors running on relative large clearance exists. This paper investigates the impact of tip leakage on the performance of centrifugal compressor systems for relative clearance ratios, ranging from 3 up to 15 %. The tip leakage analysis is conducted numerically on an experimentally validated centrifugal compressor system operating with refrigerant R134a. In order to investigate the behavior of the compressor by altering its clearance ratio, impellers with different blade heights are used to adjust the tip gap. The change in efficiency is investigated and empirical correlations available in literature are assessed. A new method to predict change in efficiency as function of relative clearance ratio is provided, thus extending current correlations to much higher relative clearance ratios.

KEYWORDS

REDUCED-SCALE CENTRIFUGAL COMPRESSOR, REFRIGERATION, TIP GAP VARIATION, NUMERICAL AND EXPERIMENTAL INVESTIGATION

NOMENCLATURE

b_1,b_2	Blade height at leading/trailing edge	[m]
c_s	Slip velocity	[m/s]
CR	Clearance ratio (t/b_2)	[-]
CFD	Computational fluid dynamics	
d_2	Impeller tip diameter	[m]
ϕ_{t1}	Global flow coefficient ($\dot{m}/(\rho_{t1} d_2^2 u_2)$)	[-]
Δh_t	Total enthalpy difference	[kJ/kg]
λ	Work input coefficient ($\Delta h_t/u_2^2$)	[-]
m	Tip clearance sensitivity	[-]
$\dot{m}$	Mass flow rate	[kg/s]
ρ_{t1}	Inlet total density	[kg/m^3]
$\eta_{pol,tt}$	Total-total polytropic efficiency ($\Psi_{pol,tt} / \lambda$)	[-]
u_2	Rotational velocity at trailing edge	[m/s]
t	Tip gap size	[m]
$\Psi_{pol,tt}$	Total-total polytropic head coefficient (y/u_2^2)	[-]
y	Polytropic work from Mallen and Saville (1977)	[kJ/kg]

INTRODUCTION

The test compressor which is part of this investigation is designed for domestic heat pump applications, requiring input power in the range of few kilowatts. As a consequence, the compressor becomes ultra-compact and a high rotational speed is needed to achieve the required pressure ratio. Compared to large-scale industrial compressors, the performance of such small compressors is deteriorated. On the one hand, this is a consequence of the lower Reynolds number occurring in smaller machines, which results in relatively higher frictional forces. On the other hand, manufacturing tolerances have a strong impact on the compressor performance. For instance, the relative shroud tip gap to ensure free spinning of the rotor, has to be larger in a reduced-scale compressor compared to an industrial one.

Applying standard design practice, new compressor design is developed beginning from reduced order models and ending in a three-dimensional numerical investigation. The starting geometry, which is obtained from a reduced order model strongly depends on the estimated compressor efficiency, thus the design process becomes iterative. A more accurate estimation of the expected efficiency is a key element to shorten the design process. Empirical correlations to estimate the expected efficiency drop due to various loss mechanisms exist and normally depend on dimensionless flow characteristics like flow coefficient or geometrical specifications. For instance, the relative tip clearance ratio at the impeller trailing edge is a commonly used metric to characterize the expected efficiency drop due to presence of a shroud tip gap. Prominent correlations which are used for such purpose are the ones by Eckert and Schnell (1961) and Pampreen (1973). They have been in use for decades, however, the validity of these correlations for reduced-scale turbomachinery has not been assessed. For instance, Sirakov (2005) suggests, that reduced-scale compressors yield increasingly penalized performance, since effects occur which are normally neglected in industrial compressors. He claims that many phenomena in reduced-scale turbomachinery have to be considered, since they have a large impact on the performance, such as high relative surface roughness, low Reynolds number flow, the shroud end-wall boundary layer effects on the tip jet and non-adiabatic conditions.

In order to assess the impact of large tip leakage on the performance and to test validity of the mentioned empirical correlations for reduced-scale centrifugal compressors, tip leakage of an experimentally investigated and numerically validated reduced-scale centrifugal compressor is investigated. The tip gap is altered numerically and its effect on performance and flow pattern is discussed. Furthermore, the sensitivity of the compressor by altering its tip gap is analyzed. A new empirical method to estimate the efficiency drop due tip leakage is provided, which enables the designer to consider tip leakage losses in the preliminary design phase, depending on the operating conditions.

TEST SETUP

The sensitivity of compressor efficiency by altering its tip gap is investigated, where a baseline case with a relative clearance ratio of 5 % at trailing edge of the impeller was experimentally investigated by Schiffmann (2009). The performance of this baseline compressor serves as the validation base for the numerical setup presented in this paper.

In a next step, the tip gap of the compressor is adjusted numerically in order to analyze the change in performance by altering its relative clearance ratio. Five different relative clearance ratios of 3 %, 5 %, 7.5 %, 10 % and 15 % are investigated, thus extending the relative tip clearance significantly compared to classical industrial scale machines.

Experimental Procedure

The investigated compressor was originally designed as a turbo compressor for a domestic heat pump processing R134a. Details about its geometry and non-dimensional design parameters are listed in Table 1. More details about the gas bearing supported compressor running at 180 krpm and its experimental investigation can be found in Schiffmann (2009, 2010, 2015).

Table 1: Main design and testing specifications

Working Fluid		[-]	R134a
Inlet conditions			
Total Pressure	p_{t1}	[bar]	1.5585
Total temperature	T_{t1}	[K]	261.71
Compressor geometry			
Tip Diameter	d_2	[m]	0.02
Main / splitter blades		[-]	9 / 9
Absolute tip clearance	t	[µm]	50
Relative tip clearance	CR	[%]	5
Outlet blade angle	β2	[°]	-50
Design conditions			
Tip speed Mach number	Ma_{u2}	[-]	1.27
Total-total pressure ratio (BEP)	Π_{tt}	[-]	2.3
Global flow coefficient (BEP)	ϕ_{t1}	[-]	0.065
Work input coefficient (BEP)	λ	[-]	0.61
Total-total polytropic head coefficient (BEP)	$\psi_{pol,tt}$	[-]	0.48
Total-total polytropic efficiency (BEP)	$\eta_{pol,tt}$	[-]	0.787
Reynolds number	Re	[-]*10^5	8.66

The compressor features an unshrouded impeller in combination with a shroud-tapered vaneless diffuser without pinch and a volute with rectangular cross section. The impeller has 9 main and splitter blades, which are backswept. The nominal tip clearance is 50 µm which corresponds to a relative clearance ratio at trailing edge of 5 %.
Experimental results have been obtained on a fully hermetic test rig. The compressor mass flow was controlled by an electrical expansion valve located downstream of the compressor, while the mass flow was measured by a Coriolis mass flow meter located between expansion valve and compressor. Overall efficiency of the compressor was determined by total temperature and total pressure probes located upstream and downstream of the compressor. The shaft speed was controlled via electric motor and drive and the total inlet conditions were kept constant (see Table 1).

Numerical Setup

A 3D approach was chosen to model the inlet, impeller and vaneless diffuser of the compressor. A passage model including main and splitter blade was selected, which corresponds to a 40° annular section of the mentioned components and decreases computational time. The 3D model was combined with reduced order models to account for the volute performance (Japikse (1996)) and the impact of disk friction (Daily and Nece (1960a, 1960b)).
Numerical simulations were performed using Numeca's multigrid flow solver Fine/Turbo (2018) in combination with interpolation tables to account for thermodynamic properties of the working fluid. For the meshing of the main-splitter blade configuration, a H-I-topology was used. Due to the low kinematic viscosity of the working fluid, a mesh size of 8 million grid points is required to properly resolve the boundary layers and to obtain a grid-independent solution. The minimum required mesh size was obtained in a grid independency study. Therefore, total-total pressure ratio and total-total polytropic efficiency was analyzed for six different mesh sizes ranging from 5 Mio. up to 16 Mio. grid points. All mesh configurations show a good prediction in terms of pressure ratio, since the lowest mesh has a deviation of less than 1 % in comparison to the highest cell count mesh. Nonetheless, the mesh size is determined by the prediction of efficiency. All mesh size bigger than

8 Mio. grid points have a deviation of less than 1 % compared to the value of the highest cell count mesh.
Numeca recommends having a non-dimensional wall distance of less than 10, in order to use a low Reynolds number turbulence model. The non-dimensional wall distance has been checked after each simulation. A maximum value of 9.8 occurred in the pressure side corner of the hub fillet at trailing edge. This value occurred for the lowest relative clearance ratio at lowest investigated mass flow rate. Nonetheless, an average non-dimensional wall distance of around 0.2 was achieved for all clearance ratios and operating points. Mesh resolution in the tip gap was set to 25 cells in spanwise direction for the baseline configuration (relative clearance ratio of 5%). The spanwise cell count for other tip gaps was adjusted to obtain a similar mesh quality as the baseline case measured by orthogonality, expansion and aspect ratio.
All end-walls are treated as adiabatic no-slip walls. Inlet boundary conditions were set via total pressure and total temperature as well as the inflow angle. Turbulence was modelled using a low Reynolds number shear stress transport approach (SST). Turbulent kinetic energy at inlet was determined based on the assumption of a turbulent intensity of 5 %. The turbulent dissipation at inlet was calculated assuming a turbulent viscosity ratio of 50 as proposed by Numeca. Similar values for the inlet turbulent dissipation rate were calculated from an estimated turbulent length scale by the authors. An averaged static pressure boundary condition was used at the outlet domain. Convergence was determined by Numecas formulation of global residual, stabilization of total pressure ratio and polytropic efficiency. The global residuum falls at part-load between three and four order of magnitudes and indicates a stable trend afterwards. At design and over-load conditions, however, a fall of four up to five orders of magnitude has been achieved before the residuum stagnates. Furthermore, mass conservation was maintained and solutions with a mass flow difference of less than 0.5 % between inlet and outlet mass flow were considered as converged. Convergence was achieved after 1000 iterations close to the design point and approximately 1300 iterations at off-design. Sufficient convergence at part-load conditions could be achieved up to around 80 % of the design mass flow rate. Operating points at lower flow rates showed periodic fluctuations in the residuum, indicating a high level of unsteadiness and are thus not closer investigated.

Validation

The quality of the numerical setup is compared to experimental data for the baseline geometry. Fig. 1 shows the compressor performance at design speed. Fig. 1a shows the total-total polytropic head coefficient, Fig. 1b the work input coefficient and Fig. 1c the total-total polytropic efficiency. Experimental data is shown as black dots, numerical results are presented as red lines with diamonds.
As can be seen from Fig. 1b, good agreement in terms of work input coefficient was achieved over the whole operating range. The virtual model provides marginally higher work input, what is mostly caused by neglecting the surface roughness and heat transfer occurring in the experiment. At maximum flow rate the virtual model deviates from the experiment. This effect can be explained by manufacturing tolerances and will be discussed more in detail below.

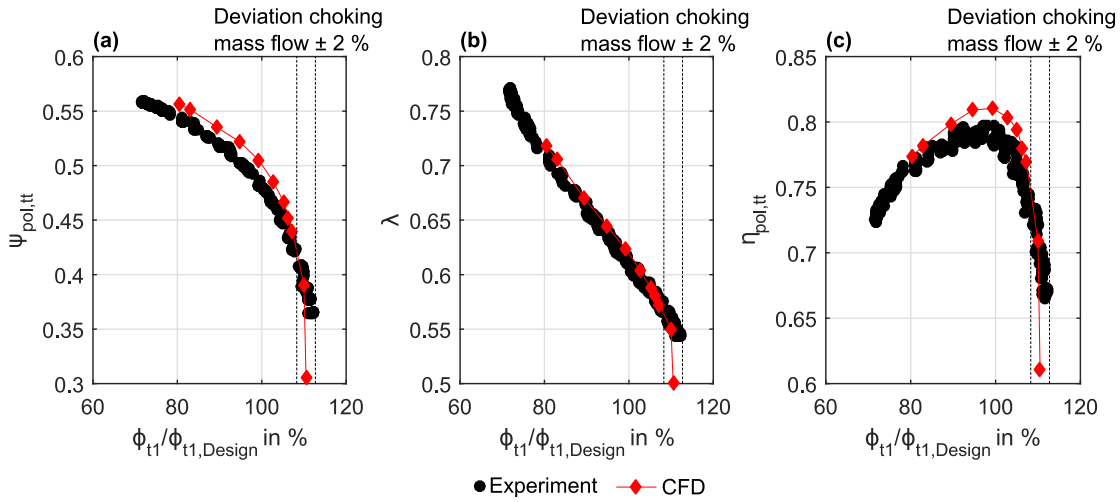

Figure 1: Total-total polytropic head coefficient (a), work input coefficient (b) and total-total polytropic efficiency (c) as function of percentage design mass flow rate.

The polytropic head coefficient shown in Fig. 1a shows a good qualitative agreement. However, numerically obtained values are consistently higher than experimental results. A contributor to the deviation could be the under-prediction of blockage in the rotor passage, leading to increased diffusion and consequently higher head. Reduced numerical blockage can source from the simplification of hydraulically smooth walls. Another contributor could be altered turbulence dissipation relative to real conditions, leading to faster mixing and decay of secondary flows in the simulation. Furthermore, inaccuracies in the reduced order volute model could contribute to deviations between model and experiment.
Polytropic total-total efficiency, shown in Fig. 1c, presents the product of head and work coefficient. As a result, the numerically obtained efficiencies yield marginally higher values over the full operating range, with a strong deterioration at choke. Qualitatively, the location of peak efficiency is well reproduced by the virtual model.
As shown in Fig. 1, simulation and experiment show a significant deviation around choke. This behavior is suggested to origin from manufacturing variations. Small errors during the flank milling process of impeller blades lead to errors in rotor throat area. As a consequence, the machine chokes at a different flow rate. In order to quantify this effect, an approach by Lüdtke (2004) to calculate choking mass flow was used and a possible difference of 2 % in throat area relative to the ideal was determined. An alteration of choking mass flow of 2 % was calculated and marked as black dashed vertical lines in Fig. 1. As can be seen, the deviation in choking mass flow between simulation and experiment lies within the manufacturing variation band. As a consequence, the choke region is excluded from the validation.
For the remaining characteristic, the virtual model provides sufficient accuracy and can be taken as validated.

Tip Gap Variation

Two possibilities can be implemented to adjust the tip gap of a centrifugal compressor. The first one is shimming the shroud end-wall linearly away from the impeller, thus the impeller geometry stays unaffected. The drawback of this approach is that only the clearance at the trailing edge is varied while the inlet clearance remains constant. In addition, the areas of other components like vaneless diffuser and volute are geometrically modified by this approach. Hence, the matching between the individual components is not necessarily given anymore.
The second approach uses impellers with different blade height to adjust the tip gap. The tip gap between impeller and housing is varied at the trailing edge as well as at the leading edge by this approach. The vaneless diffuser and the volute are geometrically unaffected.

Since the second tip gap adjustment approach is closer to the design process of a centrifugal compressor, the second approach is investigated in this paper. Five different relative clearance ratios are investigated which corresponds to 3 %, 5 % 7.5 %, 10 % and 15 % relative clearance ratio at trailing edge.

IMPACT ON THE COMPRESSOR PERFORMANCE

Non-dimensional compressor performance is fully described by the compressors flow coefficient, its rotational Mach number as well as its head and work input coefficient. The effect of altering the tip gap on the polytropic total-total head coefficient, the work input coefficient and the polytropic total-total efficiency is presented in Fig. 2 as function of the global flow coefficient. All the speed lines presented in that paper are evaluated at design speed of Ma_{u2}=1.27 and are shown for the relative clearance cases 3 % (red diamonds), 5 % (black circles), 7.5 % (blue squares), 10 % (green triangular) and 15 % (magenta diagonal triangular). The color code is kept for the remainder of that paper. The evaluation is done from compressor inlet to the outlet domain of the vaneless diffuser, in order to reduce the impact on the results of the volute model by Japikse. The polytropic work to define the polytropic head coefficient is calculated according the approach of Mallen and Saville (1977).

The polytropic head coefficient (Fig. 2a) decreases for increased relative clearance ratios, since the power loss of tip leakage is directly proportional to the tip leakage mass flow, which increases due to the area increase of the tip gap.

The work input coefficient (Fig. 2b) decreases for increased relative clearance ratios. This is mainly caused by (1) the increased blockage due to interaction of the stronger tip jet and tip leakage vortex with the main flow and (2) an increased slip velocity at trailing edge, which is caused mostly by the higher tip leakage blockage at trailing edge.

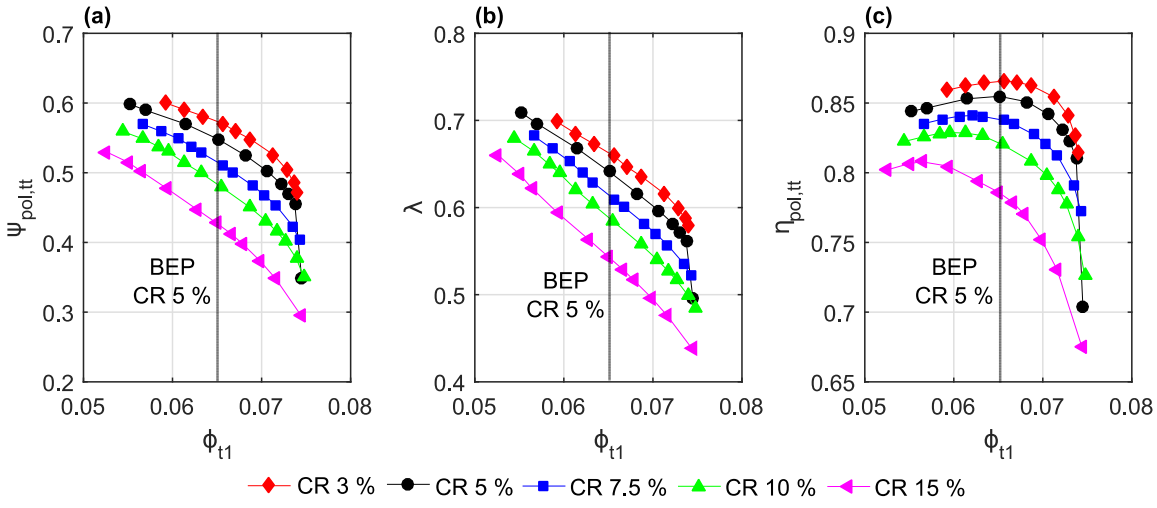

Figure 2: Total-total polytropic head coefficient (a), work input coefficient (b) and total-total polytropic efficiency (c) as function of global flow coefficient for various relative clearance ratios

The polytropic efficiency (Fig. 2c) decreases with an increase of relative clearance ratio. The peak efficiency points for each tip clearance case are shifted towards lower flow coefficients for increased relative clearance ratios, caused by the stronger blocking effect of tip leakage vortex and tip leakage jet.

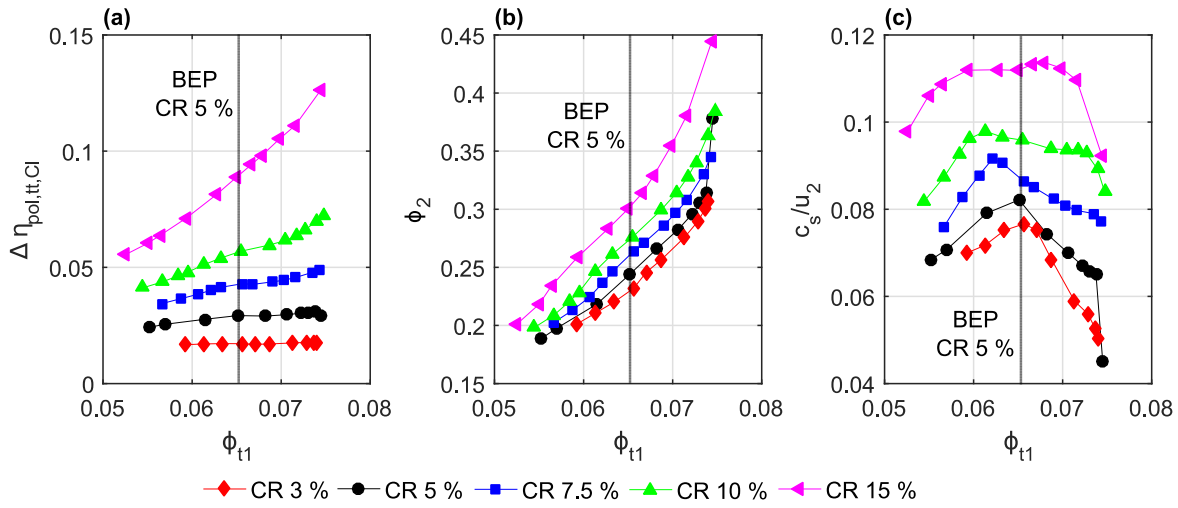

Figure 3: Drop in polytropic efficiency due to tip leakage (a), tip flow coefficient (b) and normalized slip velocity (c) as function of the global flow coefficient

Fig. 3a illustrates the loss in efficiency due to tip leakage jet as function of the global flow coefficient, assuming that all kinetic energy of the tip leakage jet at the suction side of main and splitter blades is lost. Therefore, the power loss related to tip leakage is evaluated according Eq. 1. A new head coefficient excluding the kinetic energy of tip jet has been calculated and the efficiency difference containing new and old head coefficient is presented in Fig. 3a. The drop in efficiency due to power loss of tip leakage increases for increased relative clearance ratios what is mainly caused by higher tip leakage mass flows due an increase in tip gap area. This loss reduces the head coefficient as demonstrated in Fig. 2a.

$$P = \frac{1}{2}\dot{m}_{Cl} w_{Cl}^{\ 2} \qquad [1]$$

Fig. 3b shows the flow coefficient at impeller trailing edge as function of the global flow coefficient for different relative clearance ratios. Blockage at trailing edge increases for increased relative clearance ratios, thus increasing the tip flow coefficient. This is a result of the larger tip vortex evolving at leading edge as well as the stronger tip jet that distorts and accelerates the main core flow.
Fig. 3c shows the slip velocity normalized by the tip velocity at trailing edge as a function of the global flow coefficient. The slip velocity increases by increasing the relative clearance ratio. This is a consequence of the increased blockage thus the flow has a higher velocity at trailing edge.
Both increased flow coefficient and increased slip velocity decrease the input power. Hence, more power is required to obtain the required Euler-Head. All the combined effects naturally deteriorate the compressor performance.
Fig. 4 shows the relative Mach number distribution at impeller trailing edge for the best efficiency points of various clearance ratios. The blocking effect of tip leakage and its vortex gets more pronounced with an increase of relative clearance ratio, what is observed by the high relative velocities occurring at the hub pressure side corner. As a consequence, diffusion in the impeller decrease with an increase of relative clearance ratio thus less pressurization is done to the fluid.

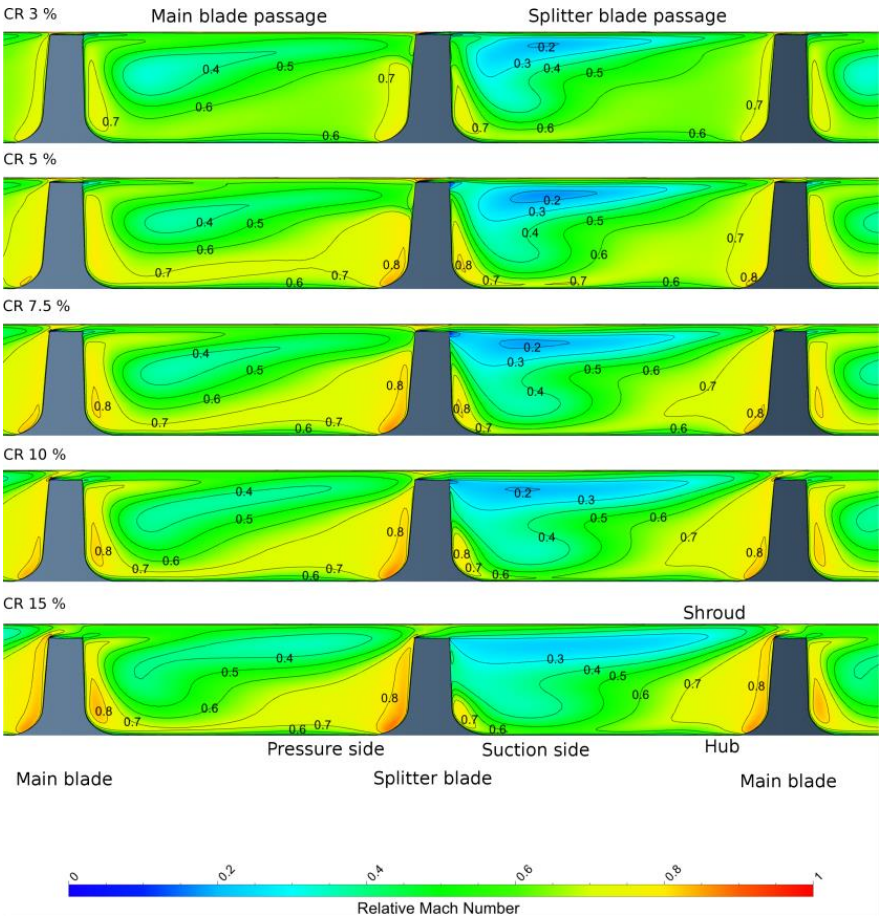

Figure 4: Relative Mach number distribution at trailing edge for various relative clearance ratios

ASSESSMENT OF EMPIRICAL CORRELATIONS

Various empirical correlations to account for a change in efficiency due to altering the tip gap are available in literature. Eckert and Schnell (1961) and Pfleiderer (1991) provided empirical correlations to estimate the deterioration of efficiency depending on the relative clearance ratio (Eq. 2). Eq. 2 offers a linear relationship between drop in efficiency and relative clearance ratio, depending on an efficiency value, which would occur at zero millimeter clearance. Senoo and Ishida (1987) suggested setting η_0 to 0.8. In order to obtain a relative clearance ratio, the absolute tip gap t is normalized by the arithmetic average of leading and trailing edge blade span $(b_1+b_2)/2$. The factor a is an empirical factor and is chosen to $a=0.9$ by Eckert and Schnell and $a=1.5$-3.0 by Pfleiderer. Eckert and Schnell (1961) provided also an empirical correlation to account for the shift in flow rate of the best efficiency point, as shown in Eq. 3.

$$\frac{\Delta\eta}{\eta_0} = -\frac{2at}{(b_1+b_2)} \qquad [2]$$

$$\frac{\Delta\phi_{t1}}{\phi_{t1,0}} = -\frac{2t}{(b_1+b_2)} \qquad [3]$$

Further correlations are the ones of Pampreen (1973) and Schmidt-Theuner and Mattern (1968). Pampreen claims, that the efficiency drop due to tip clearance is zero up to a relative clearance ratio of 3%, which motivated the author to take a relative clearance ratio of 3% as the lowest investigated value.

Fig. 5a shows the drop in efficiency obtained by the CFD setup as a function of the relative clearance ratio and compares it to the prediction of the various empirical correlations. The literature is not coherent with regards to the operating conditions at which the empirical correlations should be evaluated. Either the global flow coefficient is kept constant or the position of the best efficiency point of each speed line is considered (see Fig. 2c). In this work, the drop in efficiency was evaluated for the design flow coefficient (ϕ_{t1}=0.065) of the baseline case and for the best efficiency points evaluated for each relative tip clearance ratio.
The investigated compressor geometry suggests a more sensitive behavior to a change of relative clearance ratio compared to most of empirical correlations. Only the correlation of Pfleiderer with *a=1.5* agrees with the expected efficiency drop. The drop in efficiency is more pronounced for the same flow coefficient as compared to the change between best efficiency points for each relative clearance ratio, what is supported by the higher slope of the efficiency drop curve shown in Fig. 5a. The change in efficiency for same flow rates shows a linear dependency on the relative clearance ratio. The change between best efficiency points suggests, that the efficiency drop is less pronounced for larger clearance ratios, since the slope decreases between a relative clearance ratio of 10 % and 15 %. This corroborates with the work by Brasz (1988). Eckert and Schnell and Pampreen claim that per percentage of clearance ratio the efficiency drops approximately by 0.3 efficiency points. However, this particular compressor shows a drop of 0.5 percent efficiency points for the best efficiency points and 0.7 percent efficiency points for the same design flow coefficient of the baseline case (Fig. 5a).
Fig. 5b shows the shift of the global flow coefficient for the best efficiency points of each clearance ratio along the design speed line obtained by CFD and compares it to the global flow coefficient shift proposed by Eckert and Schnell (Eq. 3). The results clearly suggest that the shift in global flow coefficient is more pronounced compared to the empirical equation. A linear approach as used in Eq. 3 does not seem to be the correct modeling approach to account for shift in flow coefficient due to alteration of the relative clearance ratio.

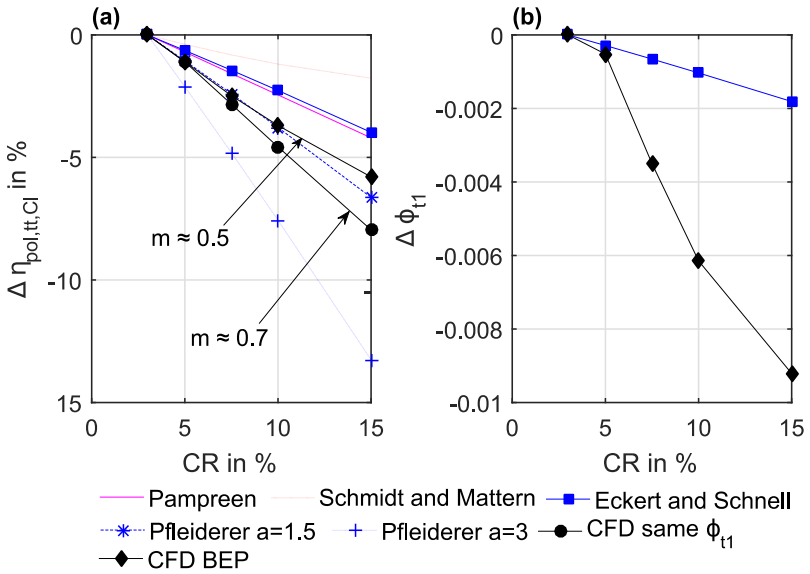

Figure 5: Drop in polytropic efficiency due to tip leakage at design flow coefficient (a) and shift of best efficiency point global flow coefficient (b) as function of relative clearance ratio

The expected efficiency drop due to tip leakage shows a dependency on both the relative tip clearance ratio *CR* and the global flow coefficient. This motivates the authors to model the efficiency drop as a linear correlation, depending on a coefficient *m* and the relative clearance ratio *CR* as described in Eq. 4, where the coefficient *m* depends on the operating point. Hence, the efficiency drop, occurring at a certain global flow coefficient, is plotted against the relative

clearance ratio and the slope of the linear relationship is calculated for each flow coefficient, starting from the lowest flow coefficient up to choke. The coefficient *m* as a function of the global flow coefficient is presented in Fig. 6.

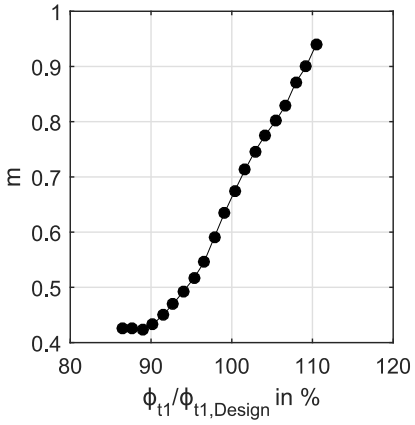

Figure 6: Sensitivity of altering the tip gap as function of percentage design flow

The sensitivity is suggested to increase with global flow coefficient, with a peak at choke. This is caused by the shift of the flow coefficient with increasing relative clearance ratio, since the choking mass flow rate is nearly constant, but the best efficiency point is shifted towards lower mass flow rates (see Fig. 2c). This leads to divergence of the curves towards higher mass flow rates.

$$\Delta\eta_{pol,tt} = -mCR \qquad 3\ \% < \mathrm{CR} < 15\ \% \qquad [4]$$

Especially in situations where the clearance ratio needs to be adapted afterward the design procedure, Eq. 4 can provide a reliable efficiency prediction without performing further calculations. For instance, the performance change due to a change of relative clearance ratio while operating - the so called running clearance – can be predicted with Eq. 4.

CONCLUSIONS AND OUTLOOK

The effect of altering the shroud tip gap was numerically investigated on a reduced-scale centrifugal compressor with an impeller diameter of 20 mm, processing R134a. The numerical model was validated by data set of an experimentally measured baseline configuration with a relative clearance ratio at impeller trailing edge of 5%.
Impellers with different blade heights were investigated numerically to adapt the relative clearance ratio, covering relative clearance ratios of 3 %, 5 %, 7.5 %, 10 % and 15 %.
By increasing the relative clearance ratio, the dimensionless compressor performance values behave as follows:

- The total-total polytropic head coefficient decreases, caused primarily by the increased tip leakage mass flow due to an area increase of the tip gap.
- The work input coefficient decreases. This is a result of the increased blockage and slip at the impeller trailing edge. Both blockage and slip increase due to a stronger tip jet and tip leakage vortex. Hence, more input power is needed to obtain the required Euler-head.
- The total-total polytropic efficiency decreases.
- The best efficiency point is shifted towards lower flow coefficients, resulting from the higher blockage at trailing edge.

The drop in efficiency depending on the relative clearance ratio has been compared to empirical correlations of Eckert and Schnell (1961), Pfleiderer (1991), Pampreen (1973) and Schmidt-Theuner and Matterrn (1968). The investigated impeller has shown a more sensitive behavior to a change of clearance ratio as suggested by these empirical correlations. Merely the correlation of Pfleiderer (1991) with a parameter choice of $a=1.5$ is in accordance with the numerical data set. A rule of thumb for this particular impeller can be stated: Increasing the relative clearance ratio by one percent yield to an efficiency drop by 0.7 efficiency points for the same flow coefficient at design point of the baseline configuration and 0.5 efficiency points for the best efficiency points of each relative clearance ratio.
This sensitivity has been analyzed along the compressors operating range. A simple equation is presented, which models the drop in efficiency as a function of the relative clearance ratio depending on the operating point.

A test-rig for testing refrigerant compressors is implemented and commissioned. Validation of the presented numerical setup with the experimental setup is one of the next steps, in order to corroborate the presented findings. Furthermore, different design strategies for tip leakage optimized impeller geometries are investigated.

ACKNOWLEDGEMENTS

The authors acknowledge the funding by the Swiss National Science Foundation, grant PYAPP2_154278/1, for financing this project. A special thank goes to Prof. M. Casey and Dr. D. Rusch for their support and contribution.

REFERENCES

Schiffmann, J., Favrat, D., (2009). *Experimental investigation of a direct driven radial compressor for domestic heat pumps*. International Journal of Refrigeration, 32(8), pp. 1918–1928.

Schiffmann, J., Favrat, D., (2010). *Design, experimental investigation and multi-objective optimization of a small-scale radial compressor for heat pump applications*. Energy, 35(1), pp. 436–450.

Schiffmann, J., (2015). *Integrated design and multi-objective optimization of a single stage heat pump turbocompressor*. Journal of Turbomachinery (ASME), 137(7), pp. 071002–071002–9.

Sirakov, B., (2005). *Characterization and design of non-adiabatic micro-compressor impeller and preliminary design of self-sustained micro engine systems*. PhD thesis, Massachusetts Institute of Technology.

Japikse, D., (1996). *Centrifugal Compressors Design and Performance*. Concepts ETI.

Daily, J., Nece, R., (1960a). *Chamber dimension effects on induced flow and frictional resistance of enclosed rotating disks*. Transactions of ASME, Journal of Basic Engineering, March, pp. 217–232.

Daily, J., Nece, R., (1960b). *Roughness effects on frictional resistance of enclosed rotating disks*. Transactions of ASME, Journal of Basic Engineering, September, pp. 553–562.

Numeca International, (2018). *Fine^{TM}/Turbo: Flow Integrated Environment*. latest ed., Numeca International, Brussels, Belgium. See also URL: http://www.numeca.com.

Mallen, M., and Saville, G., (1977). *Polytropic processes in the prediction of centrifugal compressors*. Institute of Mechanical Engineers(C183/77), pp. 89–96.

Lüdtke, K., (2004). *Process Centrifugal Compressors: Basics, Function, Operation, Design, Application*. Springer.

Eckert, B., Schnell, E., (1961). *Axial -und Radialkompressoren*. Springer.

Pfleiderer, C., Petermann, H., (1991). *Strömungsmaschinen*. Springer.

Senoo, Y., and Ishida, M., (1987). *Deterioration of compressor performance due to tip clearance of centrifugal impellers*. Transactions of ASME: Journal of Turbomachinery, 109, January, pp. 55–61.

Pampreen, R., (1973). *Small turbomachinery compressor and fan aerodynamics*. Transactions of ASME: Journal of Engineering for Power, 95, July, p. 251.

Schmidt-Theuner, P., Mattern, J.,(1968). *The effect of Reynolds number and Clearance in the centrifugal compressor of turbocharger*. The Brown-Boveri Review, Vol 55, No 8, 453-456.

Brasz, J., (1988). *Investigation into the effect of tip clearance on centrifugal compressor performance*. ASME - Gas Turbine and Aeroengine Congress, Amsterdam, Netherlands, June 6-9.